Parametric sensitivity for large-scale aeroacoustic flows

By M. Fosas de Pando†, P.J. Schmid‡ AND S.K. Lele

Even though the use of adjoints in flow optimization and control design is becoming more commonplace, their application to parameter studies is far less established. In this study, we introduce a framework for the computation of gradients of user-defined output variables with respect to governing parameters. By identifying appropriate terms of the governing equations and using them as weight operators in a scalar product between direct and adjoint solutions, gradient information, and thus sensitivity information, can be gained. The methodology is applied and illustrated on a tonal noise problem, where the change of the frequency response with respect to frequency, Mach number, and Reynolds number is determined from direct and adjoint variables. In the case of Mach number changes, the characteristic peak switching in the frequency response can be recovered.

1. Introduction

As high-performance computational resources are becoming more readily available and large-scale simulations of complex flows are becoming more feasible, optimization studies are progressively being incorporated into the analysis and manipulation of fluid flows of practical interest. Recent developments in mathematical tools and algorithmic implementation have helped advance sophisticated techniques for the quantitative analysis of fluid systems. Despite remarkable progress on many fronts, currently available algorithms for optimization, such as iterative gradient-based techniques, are still computationally expensive, and, particularly for large-scale calculations, optimal solutions—e.g. control strategies (Kim *et al.* 2014), geometric design (Walther & Nadarajah 2013), frequency responses (Garnaud *et al.* 2013), etc.—can only be computed for a rather limited number of parameter choices. For the specific case of aeroacoustic flows, these limitations are further aggravated by the inherent disparity in the spatiotemporal scales of acoustic and hydrodynamic processes, which greatly increases the cost of each iteration during the optimization process. As a consequence, the cost associated with the assessment of the parametric sensitivity of optimal solutions far exceeds typically available computing resources.

In this study, we focus on the parametric sensitivity of the frequency response of a linearly (globally) stable, compressible flow. More specifically, we consider the tonal noise problem of flow around an airfoil (Paterson *et al.* 1973; Arbey & Bataille 1983; Nash *et al.* 1999; Desquesnes *et al.* 2007; Fosas de Pando *et al.* 2014) — an acoustic phenomenon consisting of a feedback loop between instabilities in the pressure- and suction-side boundary layers, noise generation near the trailing edge, and repeated triggering of boundary-layer instabilities by upstream propagating acoustic waves. The frequency response analysis computes the optimal (i.e., maximal) gain in energy from a time-harmonic source; it

† Department of Mechanical Engineering and Industrial Design, Universidad de Cádiz, Spain
‡ Department of Mathematics, Imperial College London, United Kingdom

has been found to most aptly characterize the input-output relation and the general fluid behavior for amplifier-type flows (Trefethen *et al.* 1993). In aeroacoustic flows, this analysis may, for example, reveal worst-case scenarios for maximal acoustic radiation, isolate locations in the computational domain where the feedback loop may be broken or weakened with the least amount of effort, and provide valuable guidance in devising control strategies for noise reduction.

Mathematically, a frequency response analysis of a flow based on an L_2-measure is equivalent to the computation of the L_2-norm of the resolvent of the linearized governing equations. The leading singular value of the resolvent comprises the maximal gain in energy between a time-harmonic forcing and the response (of the same frequency) (Schmid 2007; Sipp & Marquet 2012). The principal right singular vector contains the optimal forcing, while the principal left singular vector contains the corresponding response. Typically, the frequency response depends on the governing parameters contained in the equation as well as the equilibrium state about which the equations have been linearized. A full analysis of a particular flow often requires the computation of the resolvent norm for a range of parameters and configurations in order to assess pertinent changes in the dominance of particular structures in different parameter regimes. These computations are rather costly, and typically only a few parameter combinations can be afforded with justifiable effort. Nevertheless, adjoint analysis provides first-order sensitivities to parameter changes at virtually no extra cost.

Frequency-response sensitivity of the incompressible Navier–Stokes equations with respect to base-flow perturbations has been considered by Brandt *et al.* (2011). In their work, they derived an analytical expression for the sensitivity of the optimal gain and demonstrated the technique on the incompressible flat-plate boundary layer. An application beyond this case, or for more general variations and objectives, has not been attempted to these authors' best knowledge.

This report is organized as follows. In Section 2 a brief exposition to the mathematical background is given, explaining optimal frequency-response analysis and presenting a perturbation approach to account for changes in parameters. The derived expressions are illustrated on the complex Ginzburg-Landau equation. The numerical details and implementation particulars are discussed in Section 3, prior to its application to the tonal noise problem in Section 4. In this case, the frequency response is computed and sensitivity/gradient information with respect to frequency, Mach number and Reynolds number is determined from direct and adjoint flow fields. The study then closes in Section 5 with concluding remarks.

2. Mathematical background

2.1. *Optimal frequency-response analysis*

We consider the long-time asymptotic response of linearized partial differential equations discretized in space and subjected to harmonic forcing. The temporal evolution of small perturbations $\mathbf{v}$ read

$$\frac{\mathrm{d}\mathbf{v}}{\mathrm{d}t} = \mathbf{A}\mathbf{v} + \mathbf{f}e^{-\mathrm{i}\omega t} \quad \text{with} \quad \mathbf{A} = \left.\frac{\partial \mathbf{F}}{\partial \mathbf{v}}\right|_{\bar{\mathbf{v}}}, \tag{2.1}$$

where $\mathbf{A}$ is the Jacobian of the right-hand-side of the discrete nonlinear equations $\mathbf{F}(\cdot)$ linearized around a suitable equilibrium point $\bar{\mathbf{v}}$, $\mathbf{f}$ is a given forcing, and ω is the angular frequency. If the operator $\mathbf{A}$ is stable, we characterize the amplification of the operator

by its asymptotic response to harmonic forcing for varying frequencies. In the long-time limit, the response reads

$$\mathbf{v} = -(\mathbf{A} + \mathrm{i}\omega)^{-1}\mathbf{f}. \tag{2.2}$$

We now seek forcings that maximize the response, as measured by an inner product $\langle \mathbf{w}, \mathbf{u} \rangle = \mathbf{w}^H \mathbf{M} \mathbf{u}$, where $\mathbf{M}$ is a positive definite weight matrix.

$$\mathbf{f}_{\max} = \arg\max_{\mathbf{f}} \frac{\| -(\mathbf{A} + \mathrm{i}\omega)^{-1}\mathbf{f} \|}{\|\mathbf{f}\|}, \tag{2.3a}$$

$$\mathbf{v}_{\max} = -(\mathbf{A} + \mathrm{i}\omega)^{-1}\mathbf{f}_{\max}, \tag{2.3b}$$

$$G_{\max} = \frac{\|\mathbf{v}_{\max}\|}{\|\mathbf{f}_{\max}\|}. \tag{2.3c}$$

It can be shown that the optima are given by the singular triplet $(\sigma_i, \mathbf{u}_i, \mathbf{v}_i)$ associated with the largest singular value of the matrix

$$\mathbf{R} = -\mathbf{L}(\mathbf{A} + \mathrm{i}\omega)^{-1}\mathbf{L}^{-1} \tag{2.4}$$

where $\mathbf{L}$ is related to $\mathbf{M}$ by the Cholesky decomposition $\mathbf{M} = \mathbf{L}^H \mathbf{L}$. The solution to the optimization problem then reads

$$\mathbf{f}_{\max} = \mathbf{L}^{-1}\mathbf{v}_1, \tag{2.5a}$$

$$\mathbf{v}_{\max} = \mathbf{L}^{-1}\mathbf{u}_1, \tag{2.5b}$$

$$G_{\max} = \sigma_1. \tag{2.5c}$$

These results can be extended to different choices of inner products for the forcing and the response; furthermore, we can introduce spatial restrictions for both the forcing location and the spatial extent where the response is sought to be maximized.

2.2. *Sensitivity analysis*

In this section we address a procedure to compute the influence of the parameters that govern operator $\mathbf{A}$ — such as the baseflow — on the optimal gain in Eq. (2.3). The operations involved in the evaluation of the resolvant operator and the optimization are computationally demanding, and we thus seek to leverage gradient information from the optimization process to gain further insight at no extra cost. Let us consider the singular value decomposition of the matrix $R = U\Sigma V^H$ and the following relations

$$Rv_i = \sigma_i u_i, \tag{2.6a}$$

$$R^H u_i = \sigma_i v_i. \tag{2.6b}$$

Changes in the singular value σ_i and corresponding singular vectors are related to perturbations in the matrix R by

$$(R + \delta R)(v_i + \delta v_i) = (\sigma_i + \delta\sigma_i)(u + \delta u_i), \tag{2.7a}$$

$$(R + \delta R)^H (u_i + \delta u_i) = (\sigma_i + \delta\sigma_i)(v_i + \delta v_i). \tag{2.7b}$$

If the perturbations are sufficiently small, we can neglect higher-order terms and arrive at

$$R\delta v_i + \delta R v_i = \sigma_i \delta u_i + \delta\sigma_i u_i, \tag{2.8a}$$

$$R^H \delta u_i + \delta R^H u_i = \sigma_i \delta v_i + \delta\sigma_i v_i. \tag{2.8b}$$

Projecting onto v_i and u_i, respectively, and recalling Eq. (2.6), the above relations read

$$\sigma_i v_i^H \delta v_i + u_i^H \delta R v_i \approx \sigma_i u_i^H \delta u_i + \delta\sigma_i, \tag{2.9a}$$

$$\sigma_i u_i^H \delta u_i + v_i^H \delta R^H u_i \approx \sigma_i v_i^H \delta v_i + \delta\sigma_i. \tag{2.9b}$$

We finally obtain

$$\delta\sigma_i \approx \mathrm{Re}\left(u_i^H \delta R v_i\right). \tag{2.10}$$

As we discuss below, depending on the application, it might not be straightforward to compute changes in δR with respect to perturbations in the parameters.

Alternatively, the sensitivity of a singular value can be related to perturbations of the inverse matrix R^{-1} by recalling that $R^{-1} = V\Sigma^{-1}U^H$. Hence

$$-\frac{\delta\sigma_i}{\sigma_i^2} \approx \mathrm{Re}\left(v_i^H \delta R^{-1} u_i\right). \tag{2.11}$$

We now apply the above relation to the matrix given in Eq. (2.4). Let α be a parameter of interest that define $\mathbf{A}$, then,

$$\frac{1}{\sigma_i^2}\frac{\partial\sigma_i}{\partial\alpha} \approx \mathrm{Real}\left\langle \mathbf{f}_i, \frac{\partial A}{\partial\alpha}\mathbf{v}_i \right\rangle \qquad \text{and} \qquad \frac{\partial\mathbf{A}}{\partial\alpha}\mathbf{v} \approx \frac{1}{\epsilon}\left(\mathbf{A}(\bar{\alpha}+\epsilon)\mathbf{v} - \mathbf{A}(\bar{\alpha})\mathbf{v}\right). \tag{2.12}$$

Furthermore, slope information for changes in the optimal gain with respect to ω reads

$$\frac{1}{\sigma_i^2}\frac{\partial\sigma_i}{\partial\omega} \approx -\mathrm{Im}\left\langle \mathbf{f}_i, \mathbf{v}_i \right\rangle. \tag{2.13}$$

The above equations show close relations between changes in the gain and changes in $\mathbf{A}$ in regions where $\mathbf{f}_{\max}$ and $\mathbf{v}_{\max}$ overlap. It should be noted that, although higher-order sensitivities can also be derived, their evaluation depends on the remaining singular vectors, which are usually not available.

2.3. *Frequency-response sensitivity of the complex Ginzburg–Landau equation*

We conclude this section by demonstrating the sensitivity analysis sketched above on the forced complex Ginzburg–Landau equation given by

$$\frac{\partial\phi}{\partial t} + U\frac{\partial\phi}{\partial x} = \mu(x)\phi + (1 + \mathrm{i}c_d(x))\frac{\partial^2\phi}{\partial x^2} + f(x)\exp\left(-\mathrm{i}\omega t\right), \tag{2.14}$$

with

$$U = 1, \qquad \mu(x) = \mu_0(1+\mathrm{i})\exp(-(x-10)^2), \qquad \mu_0 = 1.8, \tag{2.15a}$$

$$c_d(x) = c_{d0}\exp(-(x-10)^2/4), \qquad c_{d0} = 0.2. \tag{2.15b}$$

The domain extends from $x = -20$ to $x = 30$ and, once discretized in space, the resulting system of ordinary differential equations can be recast in the form given in Eq. (2.1). With the chosen parameters, all eigenvalues of $\mathbf{A}$ are stable, and the optimal frequency response analysis applies.

For the given matrix sizes (512×512), standard routines can readily be used to compute the leading singular values of the matrix given in Eq. (2.4). In Figure 1(a), the optimal gain for varying frequencies is represented showing maximum amplification at $\omega_{\max} \approx 1.55$. For this frequency, the optimal forcing, optimal response and their overlap is depicted in Figure 1(b).

Although for this case a sufficient number of frequencies ω can be considered, for large-scale calculations it can no longer be afforded computationally, and the optimal gain can

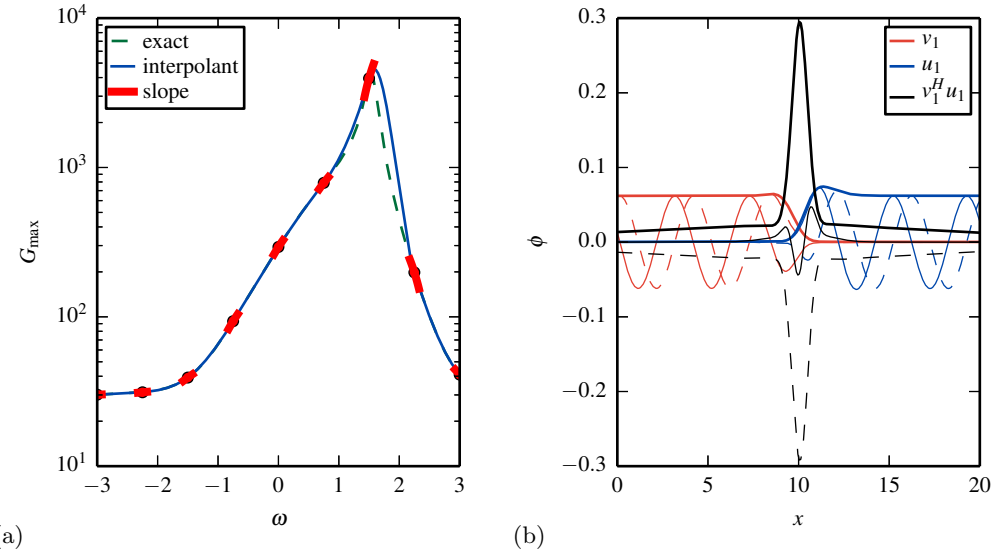

FIGURE 1. (a) Maximum gain for varying frequencies for the Ginzburg–Landau equation, (b) Optimal forcing at the peak $\omega \approx 1.55$, response and overlap between the forcing and the response. The thick, thin and dashed lines represent, respectively, the amplitude, the real and the imaginary parts.

only be computed at a signficantly reduced number of frequencies ω. Taking into account the slope information from Eq. (2.13), we represent, in Figure 1(a), a piecewise polynomial interpolant based on the optimal gain, and the first-order derivative for nine values of the frequency ω.

Using Eq. (2.12), we can now proceed to compute the sensitivity of the optimal gain $G_{\max}$ with respect to changes in parameters. In Figures 2(a–d), we display the sensitivity with respect to the advection speed $\partial_U G_{\max}(\omega)$, the instability parameter $\partial_{\mu_0} G_{\max}(\omega)$ and the dispersion coefficient $\partial_{c_{d0}} G_{\max}(\omega)$ computed with the first-order sensitivity relation given in Eq. (2.12). The first-order approximation of the changes in the optimal gain are in excellent agreement with the exact change.

3. Numerical methods

In the results presented below, we have used a direct numerical simulation code based on the compressible Navier–Stokes equations. The governing equations have been implemented using a pseudo-characteristics formulation; the discretization in space and in time has been performed using high-order compact schemes and a low-storage Runge–Kutta scheme, respectively. In addition, the numerical code features an efficient extraction technique for gaining access to the linearized direct and adjoint operators (Fosas de Pando *et al.* 2012), denoted by $\mathbf{A}$ and $\mathbf{A}^*$.

It should be noted that the evaluation of the resolvent operator in Eq. (2.4) and its adjoint requires the solution of a large-scale linear system, which is untractable for high degree-of-freedom simulations and typically available computational resources. Instead, we opt for a matrix-free iterative approach and approximate the asymptotic response by the long-time integration of Eq. (2.1). The evaluation of Eq. (2.2) has been performed using the exponential Krylov time-integration technique described in Sidje (1998). The

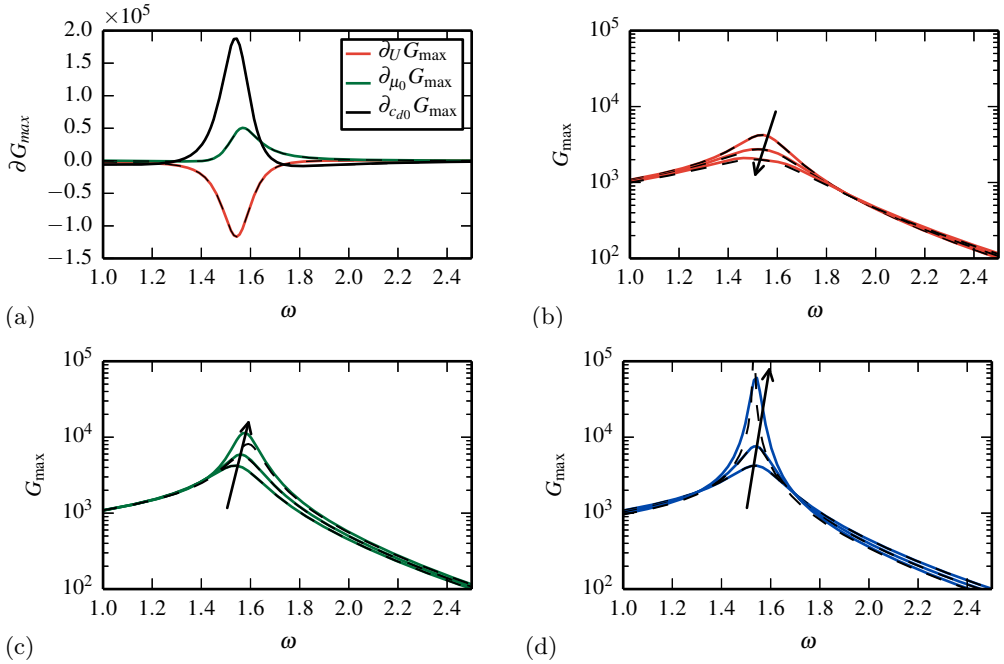

FIGURE 2. Complex Ginzburg–Landau equation: (a) sensitivity of the optimal gain $\partial.G_{\max}(\omega)$ with respect to parameters. First-order estimation of the optimal gains for changes (b) the advection speed, (c) instability coeffient μ_0, and (d) the dispersion coefficient c_{d0}. The continuous and the dashed lines represent the frequency response computed using, respectively, the first-order sensitivity relations and the exact calculations.

leading singular triplet has been computed using an iterative Lanczos technique as implemented in the software package SLEPc (Hernandez *et al.* 2005), which requires the evaluation of matrix-vector products involving the operator given in Eq. (2.4) and its adjoint.

4. Application to tonal noise in the flow around an airfoil

In this section we demonstrate the parametric sensitivity analysis on the tonal noise generated by the flow around an airfoil. We consider the two-dimensional flow around a NACA0012 airfoil section at 2^o angle of attack; the chord-based Reynolds number Re is $2 \cdot 10^5$, the Mach number M is 0.4, the heat capacity ratio γ is 1.4, and we have taken the Prandtl number Pr as 0.71. The interested reader is referred to Fosas de Pando *et al.* (2014) for details about the numerical grids, the nonlinear simulations, and a modal stability analysis. The instantaneous dilatation field, shown in Figure 3, displays strong acoustic radiation, emanating from a dipolar source near the trailing edge at a characteristic wavelength, as well as quasi-periodic vortices shedding from the near wake.

For this parameter choice, the far-field pressure spectrum is characterized by strong equally-spaced peaks. An explanation for the occurrence of discrete tones relies on a phase condition between amplified hydrodynamic instabilities along convectively unstable boundary layers and separated shear layers, and the upstream propagating acoustic waves that are generated by the passage of such instability waves over the trailing edge of the airfoil.

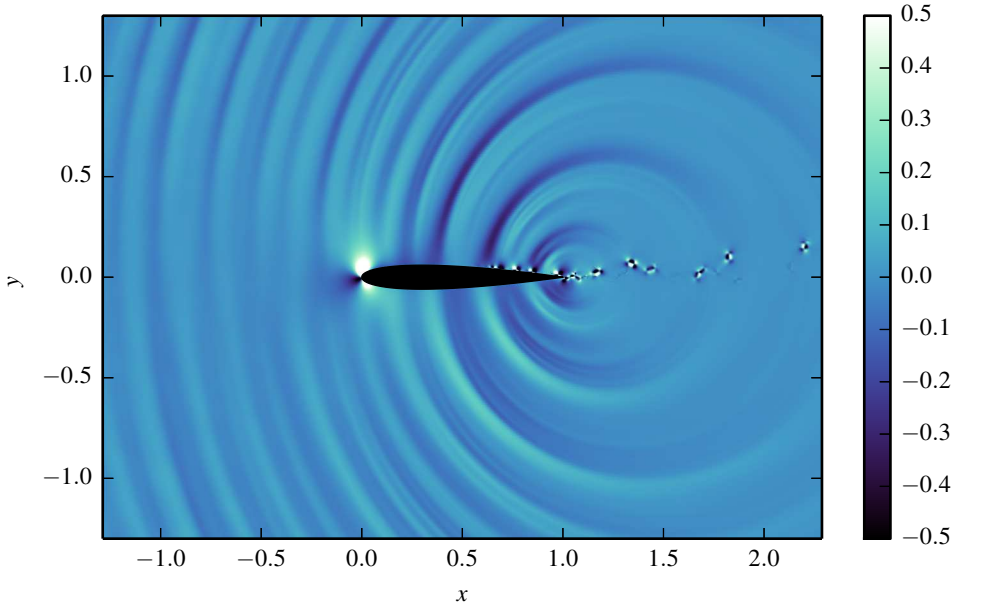

FIGURE 3. Tonal noise in the flow around an airfoil showing instantaneous dilatation field, in nondimensional units, from the nonlinear simulations (reprinted with permission from Fosas de Pando *et al.* (2014)).

Significant experimental work has shown that as the freestream velocity is increased Paterson *et al.* (1973); Arbey & Bataille (1983); Arcondoulis *et al.* (2013), the frequency of the strongest tone in the acoustic spectrum follows a ladder structure, i.e., the frequency repeatedly increases first continuously with the freestream velocity and then suddenly undergoes a discrete jump. In Fosas de Pando *et al.* (2013), the optimal frequency-response analysis has been performed on the averaged flow from nonlinear simulations, and it has been shown that, although the largest response, depicted in Figure 4(d), represents hydrodynamic features in the suction surface, the near wake and the acoustic radiation in the far field,

the optimal forcing, shown in Figure 4(c), is located upstream the separated region on the pressure surface. It is demonstrated that the frequencies of the tones in the two-dimensional nonlinear simulations are highly correlated with the frequencies at which the optimal gain exhibit local maxima; see Figure 4(b). The calculation of the optimal frequency-response presented was performed for twenty different values of the frequency ω in the range where discrete peaks appear in the nonlinear simulation. The number of degrees of freedom in the optimization problem is 5.89 million, and each calculation required approximately 6 000 CPU hours, yielding a total of 120 000 CPU hours for a single choice of freestream conditions.

Additional information on the frequencies at which gain optima occur can be gained using Eq. (2.13). This relation allows us to compute how changes in ω translate into changes in the optimal gain without the need of additional calculations. In Figure 5(c), the optimal gain for varying ω has been approximated by a piecewise interpolant where the slopes at the computed values of ω are enforced.

Parametric studies involving changes in the Reynolds number Re and Mach number M are used to investigate if a ladder structure can be accommodated within a resolvent

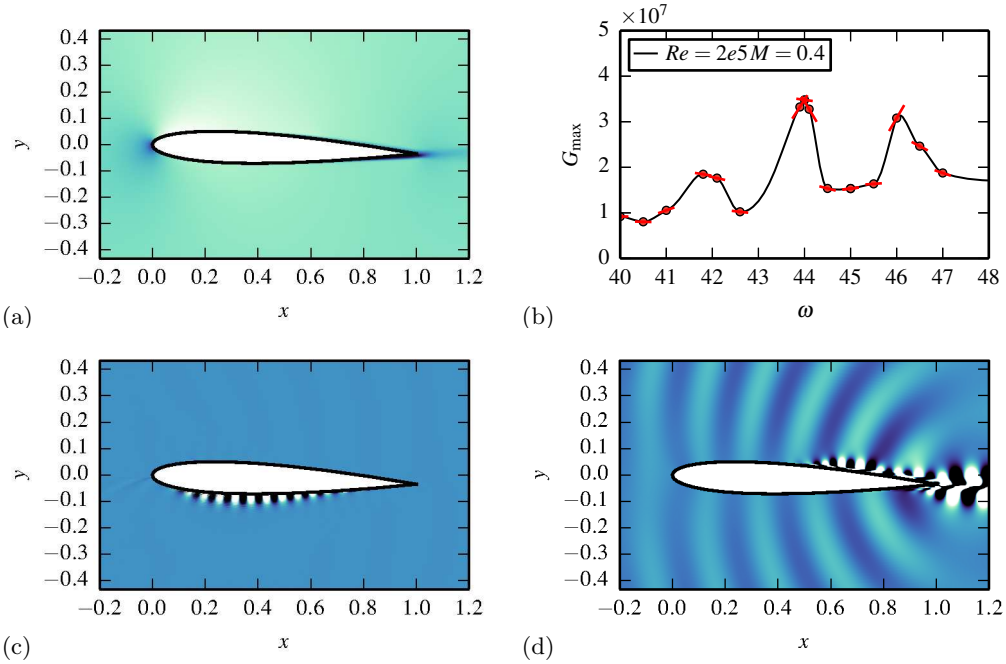

FIGURE 4. Tonal noise in the flow around an airfoil showing (a) streamwise velocity component of the time-averaged flow, (b) optimal gain for various frequencies and piecewise interpolation using slope information, (c) optimal forcing at the peak $\omega = 44$ (in nondimensional units), and (d) the associated optimal reponse.

analysis framework. With the given computational cost for a single parameter choice, wide-ranging parametric studies seem prohibitive, and we thus contend with the first-order sensitivity analysis presented in section 2.

We then proceed, using Eq. (2.12), to compute sensitivities of the optimal gain with respect to the Reynolds number and the Mach number. The Reynolds number sensitivity in Figure 5(a) reveals that the optimal gain at the peaks in 5(a) decreases as the Reynolds number is increased; on the other hand, the frequencies at which the peaks occur remain practically constant. The sensitivity analysis with respect to changes in the Mach number (Figure 5(b)) shows that all peaks are highly sensitive: the frequency of the peaks increases with the Mach number, the peaks at $\omega \approx 42$ and $\omega \approx 44$ increase, whereas the amplitude of the peak at $\omega \approx 46$ is reduced as the Mach number increases. Although differences with experimental observations remain visible, the main features of tone noise are observed: frequency increase with respect to freestream velocity and switching between consecutive peaks. A detailed comparison between the results presented in this work and experimental results will be the subject of future investigations.

It is worth recalling that the first-order approximation of the changes in optimal gain with respect to parameter changes is obtained using exclusively the gradient information gathered during the optimization process: (i) the optimal forcing, (ii) the optimal response and (iii) the changes in the operator $\mathbf{A}$. With the techniques employed in this work, the computational cost is comparable to that of an evaluation of the right-hand-side of the nonlinear equations, which is often considered negligible.

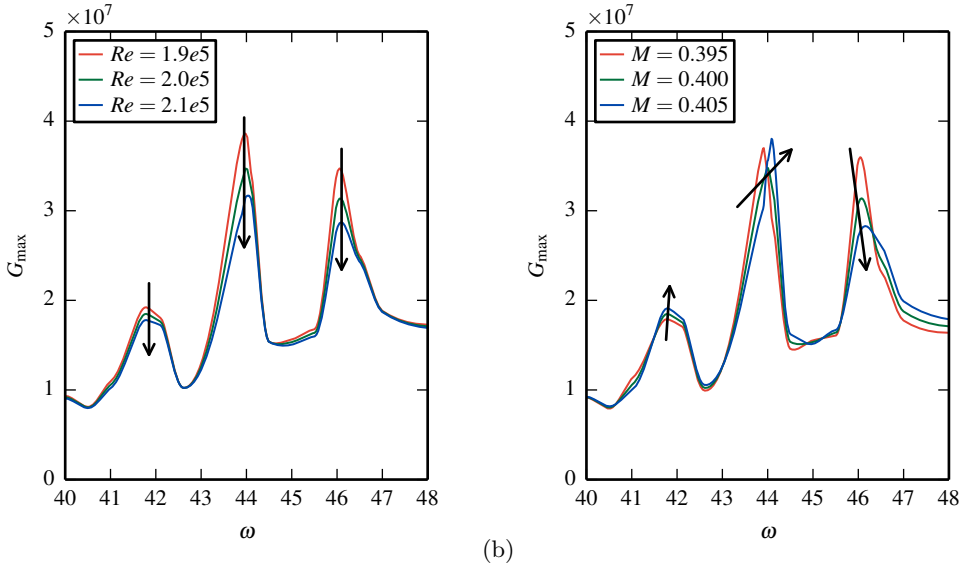

FIGURE 5. Sensitivity of the optimal gain in the tonal noise problem with respect to changes in (a) Reynolds number, (b) Mach number. See text for further details.

5. Summary and outlook

This study has introduced a numerical framework for the calculation of parameter sensitivities based on direct and adjoint flow fields. A perturbative approach has been taken to derive expressions for the first-order derivatives of singular values (describing the frequency response in our case) with respect to governing parameters or the frequency itself. Gradient information with respect to frequency can be used to apply cubic-Hermite interpolation to the frequency-response curve at the selected frequencies and thus obtain a more accurate and well-resolved representation across the computed frequency range. Gradient information with respect to governing parameters (in our case, the Mach and Reynolds numbers) gives details about changes in the response behavior as these parameters are varied. This information, however, is obtained without computing frequency responses at different values of these parameters; it simply results from a judicious evaluation of already computed (direct and adjoint) flow fields at virtually no additional cost.

The framework developed above can straightforwardly be applied to objectives other than the frequency response and to changes other than governing parameters. In this sense it represents an effective computational structure to obtain a maximum amount of information from available flow fields. Combined with an efficient extraction technique for linearized and adjoint data from nonlinear compressible flow solvers (Fosas de Pando *et al.* 2012), it provides a more encompassing manner of quantitatively analyzing complex parameter-dependent flows.

Acknowledgments

The authors acknowledge the stimulating and supportive environment at CTR during the 2014 Summer Program; in particular, we wish to thank the members of the aeroacoustic noise group for their encouraging feedback and many fruitful discussions.

REFERENCES

Arbey, H. & Bataille, J. 1983 Noise generated by airfoil profiles placed in a uniform laminar flow. *J. Fluid Mech.* **134**, 33–47.

Arcondoulis, E. J., Doolan, C. J., Zander, A. C. & Brooks, L. A. 2013 An experimental investigation of airfoil tonal noise caused by an acoustic feedback loop. In *Proceedings of Acoustics 2013*, Australian Acoustical Society.

Brandt, L., Sipp, D., Pralits, J. & Marquet, O. 2011 Effect of base-flow variation in noise amplifiers: the flat-plate boundary layer. *J. Fluid Mech.* **687**, 503–528.

Desquesnes, G., Terracol, M. & Sagaut, P. 2007 Numerical investigation of the tone noise mechanism over laminar airfoils. *J. Fluid Mech.* **591**, 155–182.

Garnaud, X., Lesshafft, L., Schmid, P. & Huerre, P. 2013 The preferred mode of incompressible jets: linear frequency response analysis. *J. Fluid Mech.* **716**, 189–202.

Hernandez, V., Roman, J. E. & Vidal, V. 2005 SLEPc: A scalable and flexible toolkit for the solution of eigenvalue problems. *ACM Trans. Math. Soft.* **31**, 351–362.

Kim, J., Bodony, D. & Freund, J. 2014 Adjoint-based control of loud events in a turbulent jet. *J. Fluid Mech.* **741**, 28–59.

Nash, E. C., Lowson, M. V. & McAlpine, A. 1999 Boundary-layer instability noise on aerofoils. *J. Fluid Mech.* **382**, 27–61.

Fosas de Pando, M., Schmid, P. & Sipp, D. 2014 A global analysis of tonal noise in flow around aerofoils. *J. Fluid Mech.* **754**, 5–38.

Fosas de Pando, M., Schmid, P. J. & Sipp, D. 2013 Tonal noise in the flow around an aerofoil: A global stability analysis. In *21ème Congrès Français de Mécanique.*

Fosas de Pando, M., Sipp, D. & Schmid, P. 2012 Efficient evaluation of the direct and adjoint linearized dynamics from compressible flow solvers. *J. Comput. Phys.* **231**, 7739–7755.

Paterson, R. W., Vogt, P. G., Fink, M. R. & Much, C. L. 1973 Vortex noise of isolated airfoils. *J. Aircraft* **10**, 296–302.

Schmid, P. J. 2007 Nonmodal stability theory. *Annu. Rev. Fluid Mech.* **39**, 129–162.

Sidje, R. B. 1998 Expokit. a software package for computing matrix exponentials. *ACM Trans. Math. Soft.* **24**, 130–156.

Sipp, D. & Marquet, O. 2012 Characterization of noise amplifiers with global singular modes: the case of the leading-edge flat-plate boundary layer. *Theor. Comput. Fluid Dyn.* **27**, 617–635.

Trefethen, L., Trefethen, A., Reddy, S. & Driscoll, T. 1993 Hydrodynamic stability without eigenvalues. *Science* **261**, 578–584.

Walther, B. & Nadarajah, S. 2013 Constrained adjoint-based aerodynamic shape optimization of a single-stage transonic compressor. *J. Turbomach.* **135**, 021017.